RSC Advances

PAPER

View Article Online
View Journal | View Issue

Cite this: *RSC Adv.*, 2026, **16**, 22470

In situ meat spoilage monitoring *via* label-free recognition of ethylenediamine using a flexible paper-based electrochemical sensor

Rokhsareh Ebrahimi,[a] Houman Kholafazad Kordasht,[b] Mohammad Hasanzadeh *[c] and Nasrin Shadjou[d]

Ethylenediamine (EDA), a primary biomarker of meat spoilage, has gained considerable attention for its potential uses in the monitoring of meat freshness. Standard analytical approaches have been widely applied for the detection of EDA, meaning that more rapid and convenient detection methods are highly desirable. Here, we introduce an innovative paper-based electrochemical sensor for label-free detection of EDA. To implement a three-electrode system on the surface of paper, silver conductive nano-ink (Ag nano-ink) was drawn by direct pen-on-paper technology. The structure, morphology, and elemental composition of the Ag nano-ink were analyzed using field-emission scanning electron microscopy and energy-dispersive spectroscopy. The presence of the target in the sensing zone changed the electrochemical signal, which was measured using square wave voltammetry. The results demonstrated that the developed sensor detected the target in a linear range from 10 to 1000 μM with a low limit of quantification of 10 μM. Interestingly, the prepared sensing approach demonstrated a strong ability to determine EDA levels in spoiled beef samples. The selectivity of the designed platform was evaluated by assessing the interference of various amino acids. In addition, the prepared paper-based sensor demonstrated excellent stability for four days. We hope that using Ag nano-ink in a novel electrochemical paper-based sensor for recognizing EDA can open a new window for detecting other biogenic amines in the future.

Received 5th January 2026
Accepted 8th April 2026

DOI: 10.1039/d6ra00092d

rsc.li/rsc-advances

1. Introduction

Food safety has gained increasing attention in recent years due to its vital role in safeguarding consumer health and its significant economic implications globally.[1] In general, meat is an essential and abundant source of protein, vitamins, and minerals needed for human growth. Meat is susceptible to spoilage during storage, and this factor must be carefully considered.[2] Recently, biogenic amines (BAs), one of the most important markers of meat spoilage, have received considerable attention. BAs are primarily produced in the meat through the enzymatic decarboxylation of amino acids. In particular, these small organic molecules demonstrate high biological activity due to their hydroxyl, aromatic, and aliphatic structural bases. Despite the important roles of some BAs in the body, excessive amounts can result in toxicity.[3–6] Ethylene diamine (EDA), one of the primary BAs, can pose potential health risks due to its toxicity. According to a report by the World Health Organization (WHO), the recommended occupational exposure limit for EDA is 10 ppm.[7]

Conventional instrumental analytical techniques based on mass spectrometry and gas chromatography have been widely used for the analysis of BAs in food.[8,9] Although these methods play a significant role in the identification of BAs, they are usually expensive, time-consuming, and require trained personnel for operation.[10] As such, inexpensive and reliable sensing devices are crucial for detecting BAs.

Electrochemical biosensors offer innovative, rapid and efficient analytical methods for monitoring of BAs. The mechanism of operation of these sensors is based on the measurement of the electrical signal generated by redox reactions of BAs at the electrode surface.[11,12] Over the past few decades, electrochemical biosensors have been designed on the surface of different electrodes, such as paper,[13] gloves,[14] leaves,[15] and disks,[16] enabling the development of portable sensing devices. Paper-based devices, in particular, are emerging analytical tools that have a high potential for cost-effective quantification of BAs in complex food matrices, especially in low-resource settings. In addition, other advantages include low materials costs, the ability to operate without the need for bulky instruments, and simple fabrication.[17,18] There have been several attempts to develop paper-based electrochemical biosensors using different

[a]Asian Nano-ink (ANI) Company, Tabriz University of Medical Sciences, Tabriz, Iran
[b]Nutrition Research Center, Tabriz University of Medical Sciences, Tabriz, Iran
[c]Pharmaceutical Analysis Research Center, Pharmaceutical Sciences Institute, Tabriz University of Medical Sciences, Tabriz, Iran. E-mail: hasanzadehm@tbzmed.ac.ir
[d]Department of Nanotechnology, Faculty of Chemistry, Urmia University, Urmia, Iran

conductive inks to facilitate sensors with excellent portability and cost-effective substrates. Among the different types of paper-based electrochemical biosensors, three-electrode systems have attracted particular attention in this field. The specific thermal and optical features of conductive inks containing silver nanoparticles (AgNPs) make them ideal sensing substrates for the portable detection of EDA.[19,20]

In this research work, we designed a novel flexible paper-based electrochemical sensor for EDA detection. For the first time, a synthesized conductive and stable Ag nano-ink based on AgNPs was used for the analysis of EDA in beef samples. To this end, the counter, reference, and working electrodes were drawn on the paper surface by a "pen-on-paper" technique to fabricate a disposable three-electrode system. Subsequently, quantitative application of the paper-based electrochemical sensor was conducted by applying a potential and measuring the voltammetric current in the sensing zone.

2. Experimental

2.1. Chemicals and reagents

All reagents and chemicals utilized in this research were of analytical grade. EDA, sodium hydroxide, silver nitrate ($AgNO_3$), potassium ferricyanide ($K_3[Fe(CN)_6]$), and potassium ferrocyanide ($K_4[Fe(CN)_6]$) were purchased from Sigma Aldrich (Ontario, Canada). Diethanolamine (DEA anhydrous, 99.5%) was used as the complexing agent and polyacrylic acid (PAA, molecular weight 450 000) was used as the stabilizer. Amino acids, including cysteine (Cys), ascorbic acid (AA), dopamine (DA), proline (Pro), aspartic acid (Asp), arginine (Arg), and glycine (Gly), as well as glucose, uric acid (UA), and urea, were purchased from Merck (Germany). Deionized water was obtained from Ghazi Pharmaceutical Company (Tabriz, Iran). Beef muscle meat samples were purchased from a local store in Tabriz, Iran.

2.2. Apparatus

FE-SEM (Hitachi SU8020, Czech operated at 3 kV) was utilized to analyze the structure, morphology, and size of the synthesized Ag nano-ink electrodes. EDS was utilized to demonstrate the chemical composition of the electrodes. A three-electrode system on photographic paper and the PalmSens 4c system were used for electrochemical detection.

2.3. Synthesis of Ag nano-ink

In this study, AgNPs were prepared based on our previous research (Fig. S1).[21] Briefly, 40 g of PAA and 915.1 g of DEA were mixed in deionized water for 2 h in a water bath. In the following steps, an $AgNO_3$ solution was added and stirred for 22 h. Subsequently, the arranged solution was sonicated for 1.5 h at 65 °C and integrated with 300 mL of ethanol and centrifuged at 9000 rpm for 20 minutes. After washing with deionized water, a 2% by weight hydroxypropyl cellulose solution in 1 : 1 (v: v) methanol and water was added to the prepared solution. Eventually, the above composite was homogenized for 3 min (Fig. S1, SI).

2.4. Preparation of the meat samples

The samples were uniformly homogenized using a food blender and fermented at room temperature for 24 h. Subsequently, 50 mg of homogenized meat was mixed with 25 mL of PBS (0.1 M, pH 7.5) solution and vortexed for 5 min. Then, EDA (50, 100, 200, 400, 600, 800, and 1000 μM) was spiked into various samples. The samples were centrifuged at 12 000 rpm for 10 min, and the supernatant was collected after filtration through a syringe filter and stored at 4 °C for subsequent use.

2.5. Fabrication of a three-electrode paper-based electrochemical sensor

The paper electrodes were assembled on photographic paper using a pen design that contained conductive Ag nano-ink, with each three-electrode paper system measuring 2 cm in length and 1 cm in width. In this substrate, the counter, reference, and working electrodes were drawn by Ag nano-ink. As shown in Fig. S2 (SI) and Scheme 1, 5 μL of EDA was incubated on the sensing zone of the working electrode through a drop casting technique (room temperature, 20 min).

3. Results and discussion

3.1. Electrochemical behavior

The electrochemical behavior of EDA on the surface of the working electrode (0.2 cm) was investigated using cyclic voltammetry (CV), SWV and DPV (Fig. 1). The standard probe solution of 5 mM $K_4[Fe(CN)_6]/K_3[Fe(CN)_6]$ (1 : 1) along with 0.005 M KCl was used as a supporting electrolyte to record the current intensity. As shown in Fig. 1A and B, the peak current intensity of the synthesized Ag nano-ink is equal to 852 μA. After incubation of EDA, the current increased to 9724 μA, which demonstrated charge-transfer kinetics rather than intrinsic conductivity or redox activity of EDA. In other words, the presence of EDA enhanced the electron transfer between the electrode and redox species, which resulted in the observed amplification of the voltammetric response (Fig. 1D–F). Notably, the increased peak current in the SWV and DPV analyses confirmed the CV results. The current intensity and potential of these methods are summarized in Table S1 (SI).

3.2. Morphological and functional characterization of the Ag nano-ink electrode

The morphology of the Ag nano-ink electrode was examined by FE-SEM and cross-sectional imaging. As shown in the FE-SEM images in Fig. 2A–F, the Ag nano-ink was uniformly distributed and immoblized on the photographic paper. In addition, as illustrated in Fig. 2A–F, the presence of silver flakes uniformly dispersed in the ink matrix was confirmed. The average diameter of the AgNPs synthesized in this work was about 58 nm. This size is important for conductive inks because particle size and uniformity are key nanoparticle parameters that influence ink stability, electrical conductivity and curing temperature. The presence of EDA influences the morphology and distribution of the AgNPs (Fig. 2G–K). Specifically, as you can see in Fig. 2G, the clustered structure confirms a successful

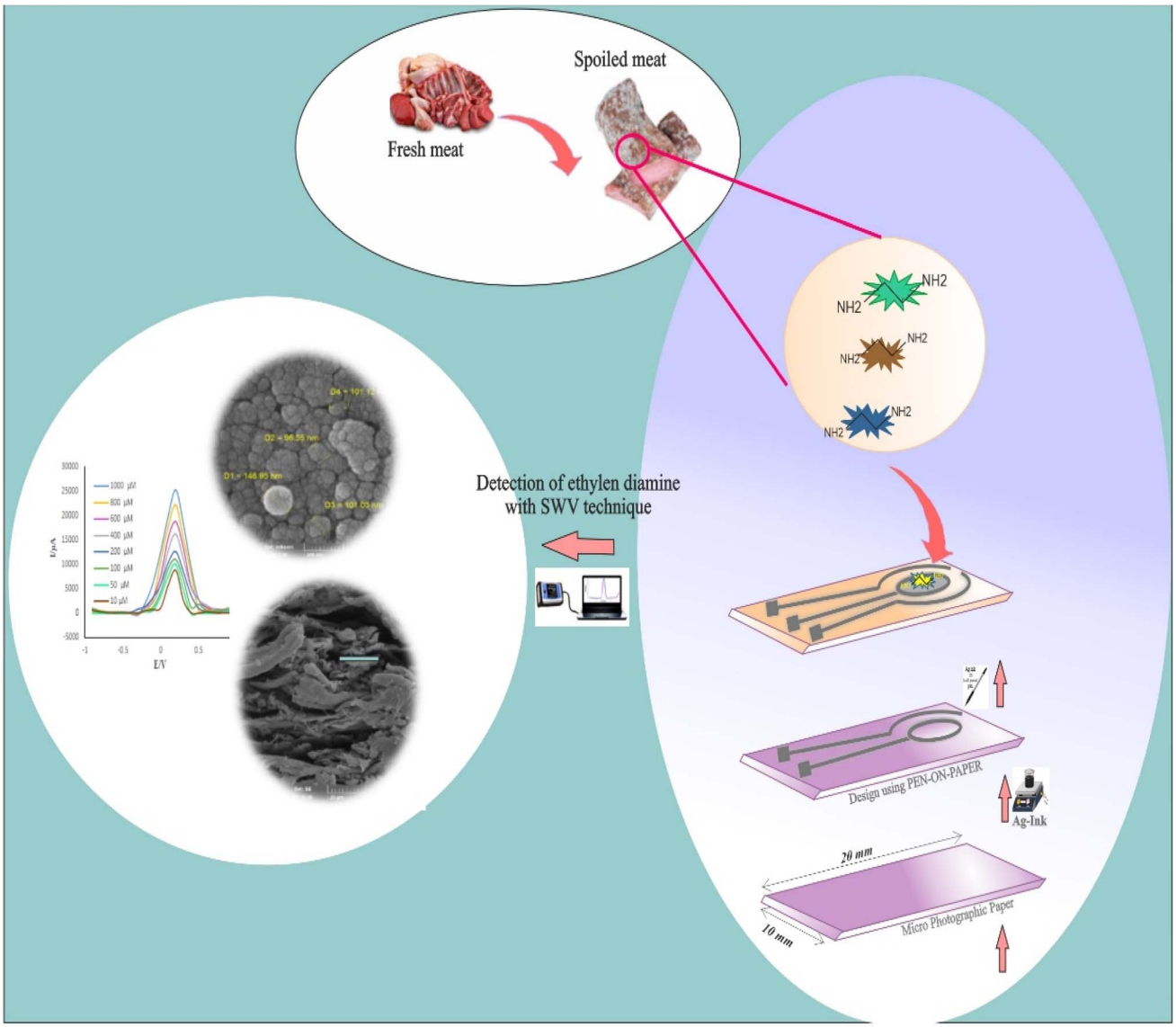

Scheme 1 EDA analysis using a paper-based electrochemical sensor prepared from silver conductive ink.

interaction. In the cross-sectional SEM images in Fig. 3A–F, the paper fibers are clearly shown. Additionally, the difference in thickness demonstrated successful modification of the photographic paper, as shown in Fig. 3A–K.

In addition, the EDS analysis revealed the strong presence of a characteristic AgLα peak at around 3 keV, which is the expected X-ray emission for Ag (Fig. 4A). In addition, the dominance of Ag in the measured area is further supported by the high intensity of the AgLα line (~1458 counts). As illustrated in Fig. 4B, the reduction in Ag signal and the emergence of nitrogen (N) demonstrated the adsorption of EDA on the Ag nano-ink.

3.3. Analytical study of the prepared paper-based electrochemical sensors

The SWV technique was used to investigate the effect that the concentration of EDA has on the current intensity. For this purpose, different concentrations of the target (10 to 1000 μM) were incubated at room temperature for 20 min. As the concentration of EDA increases, the current intensity was enhanced (Fig. 5A and B). The linear regression equation obtained from the analysis is as follows: I_P (μA) = 16.238C_{EDA} + 9185.1, R^2 = 0.9971. This confirms the accuracy of the sensor performance based on the bright signal. The developed paper-based sensor exhibited a LLOQ of 10 μM. A comparison of the performance of the developed paper-based electrochemical sensor with other analytical approaches is summarized in Table 1.

Table 1 compares the analytical performance of different methods for the detection of EDA in different matrices. Although fluorescence-based methods have high sensitivity with very low detection limits (in the nanomolar range) and good linear ranges, they often require complex equipment and transparent samples and may be affected by optical

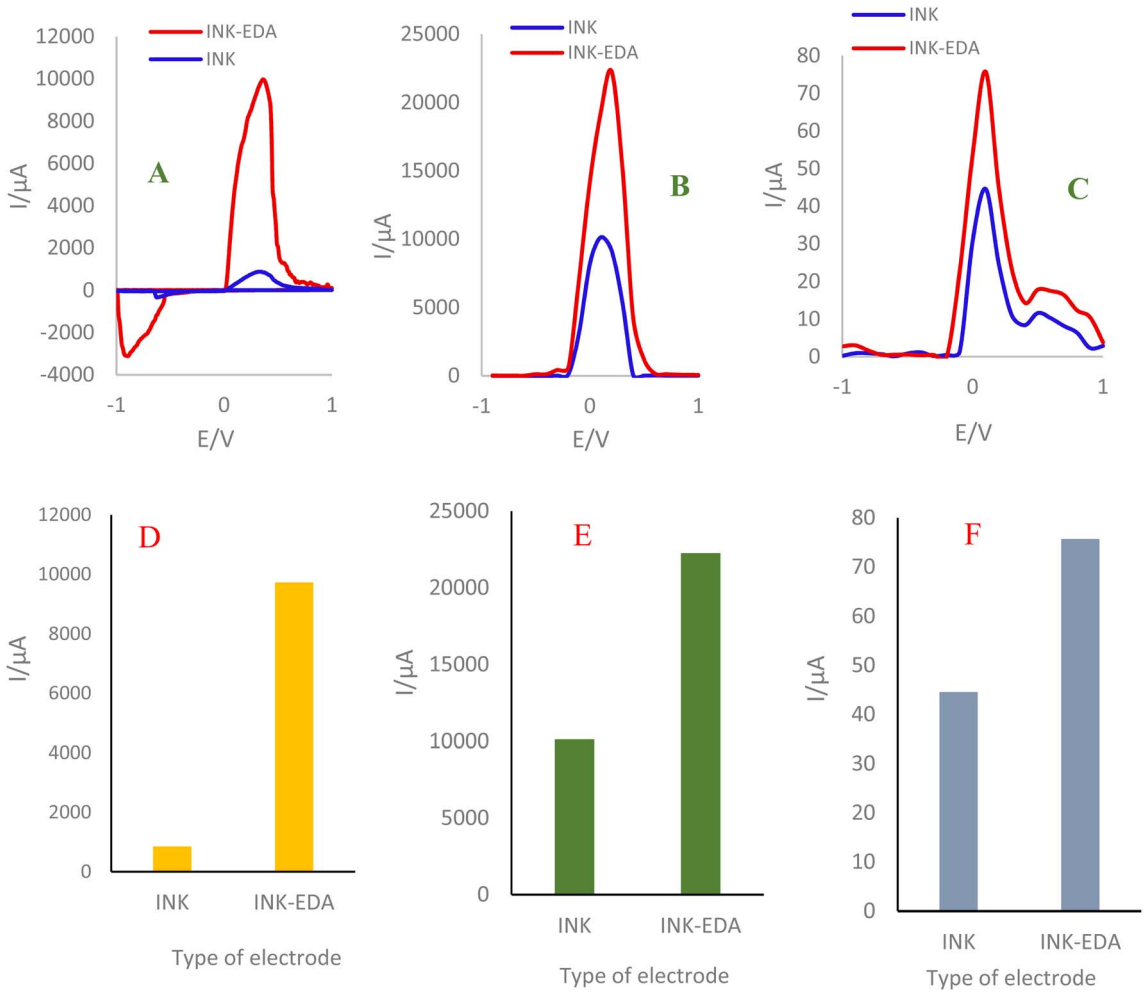

Fig. 1 (A–C) CV, SWV, and DPV of the paper-based electrochemical sensor with/without EDA in the presence of ferrocyanide/ferricyanide/KCl (5 mM) over the potential range of −1 to +1 V. (D–F) Related histograms of the results shown in (A–C).

interference. Chemiresistive methods also show good sensitivity and are suitable for gas sensing, but usually have lower selectivity in complex environments. The other electrochemical methods reported in the table display a range of sensitivities (from nanomolar to micromolar) and linear ranges, indicating the versatility of these methods for different analytical purposes. The electrochemical method presented in this study, with a detection limit of 10 μM and a linear range of 10–1000 μM, is considered a method with moderate sensitivity compared to highly sensitive methods such as fluorescence sensing (nanomolar). However, the sensor developed in the current study has major advantages, including simplicity and cost-effectiveness of the equipment, resistance to sample opacity or color effects, fast response, and real-time monitoring capability. It also has the potential to be miniaturized and integrated into advanced sensing platforms. In contrast, its main limitations are lower sensitivity than some methods, a relatively limited linear range, and the possibility of interference from electroactive species in complex matrices. This method is suitable for practical applications that require rapid, low-cost, and reliable measurements in the mentioned concentration range (such as in industrial monitoring).

3.4. Beef sample analysis

The SWV technique was used to evaluate the feasibility of the proposed platform for the detection of EDA in beef samples (Fig. S3 (SI)). For this purpose, the extracted meat sample was mixed with varied concentrations of EDA (50, 100, 200, 400, 600, 800, and 1000 μM) (v/v) and incubated on the surface-modified sensing zone. The SWV results at various concentrations of EDA in beef samples are shown in Fig. 5. The intensity of the peak increased with increasing concentration of the target analyte. Under optimal conditions, the obtained LLOQ and linear range were 10 μM and 50 to 1000 μM, respectively. The calibration curve plotted with the linear regression equivalence obtained from the SWV analysis of the beef samples is as follows: $I\,(\mu A) = 5.2627C_{EDA}\,(\mu M) + 1791.9$, $R^2 = 0.9954$.

3.5. Selectivity of the paper-based electrochemical sensor

To investigate the ability of the developed paper-based electrochemical sensor for detecting EDA, several interferers, such as Cys, AA, DA, UA, Pro, ASP, Met, Arg, Gly, urea and glucose, that are present in real beef samples were introduced. According to the SWV results in Fig. S4 (SI), the current of the designed

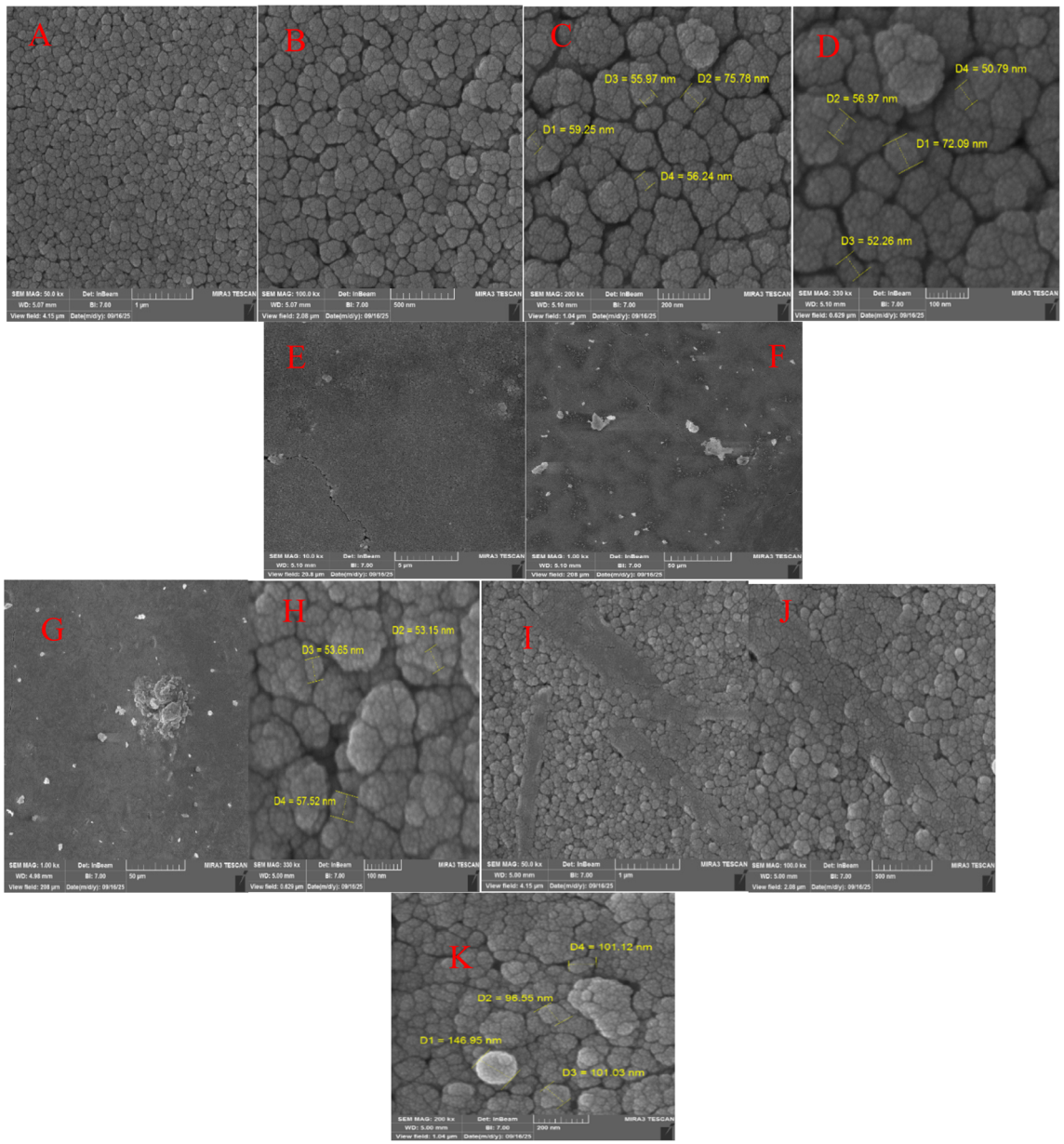

Fig. 2 (A–F) FE-SEM images of the Ag nano-ink on the surface of photographic paper. (G–K) FE-SEM images of the EDA/Ag nano-ink on the surface of photographic paper at different magnifications.

electrochemical sensor is approximately equal to 10 949 μA, which is drastically reduced in the presence of the interferers. The difference in the current intensity of the paper-based electrochemical sensor in the presence of different interferers is summarized in Table S2 (SI).

The results in Table S2 (SI) demonstrate that the sensor shows a significant electrochemical response to EDA, while the response to the other tested species is very small. The peak current (I_p) recorded for pure EDA was about 10 949 μA, while this value was significantly lower for mixtures of EDA with each of the interfering species (*e.g.*, it decreased to 3005 μA for EDA + Cys). This observation confirms that even in the presence of equivalent or higher concentrations of interfering species, the sensor has a clear tendency to interact with the target EDA. The possible mechanism of this selectivity can be attributed to the specific nature of the interaction between the amine groups of EDA and the surface of the silver nanoparticles in the conductive ink structure. The primary amine groups of EDA, probably through dative interactions with silver, allow for stronger binding and more efficient electron transfer compared to other amino acids (which have different functional groups or different ester positions). Furthermore, the peak oxidation potential for EDA was observed at around 0.2 V, which was different from the potentials recorded for most interfering species (generally in the range of 0.3 to 0.4 V). This potential separation also helps to distinguish the EDA signal from that of

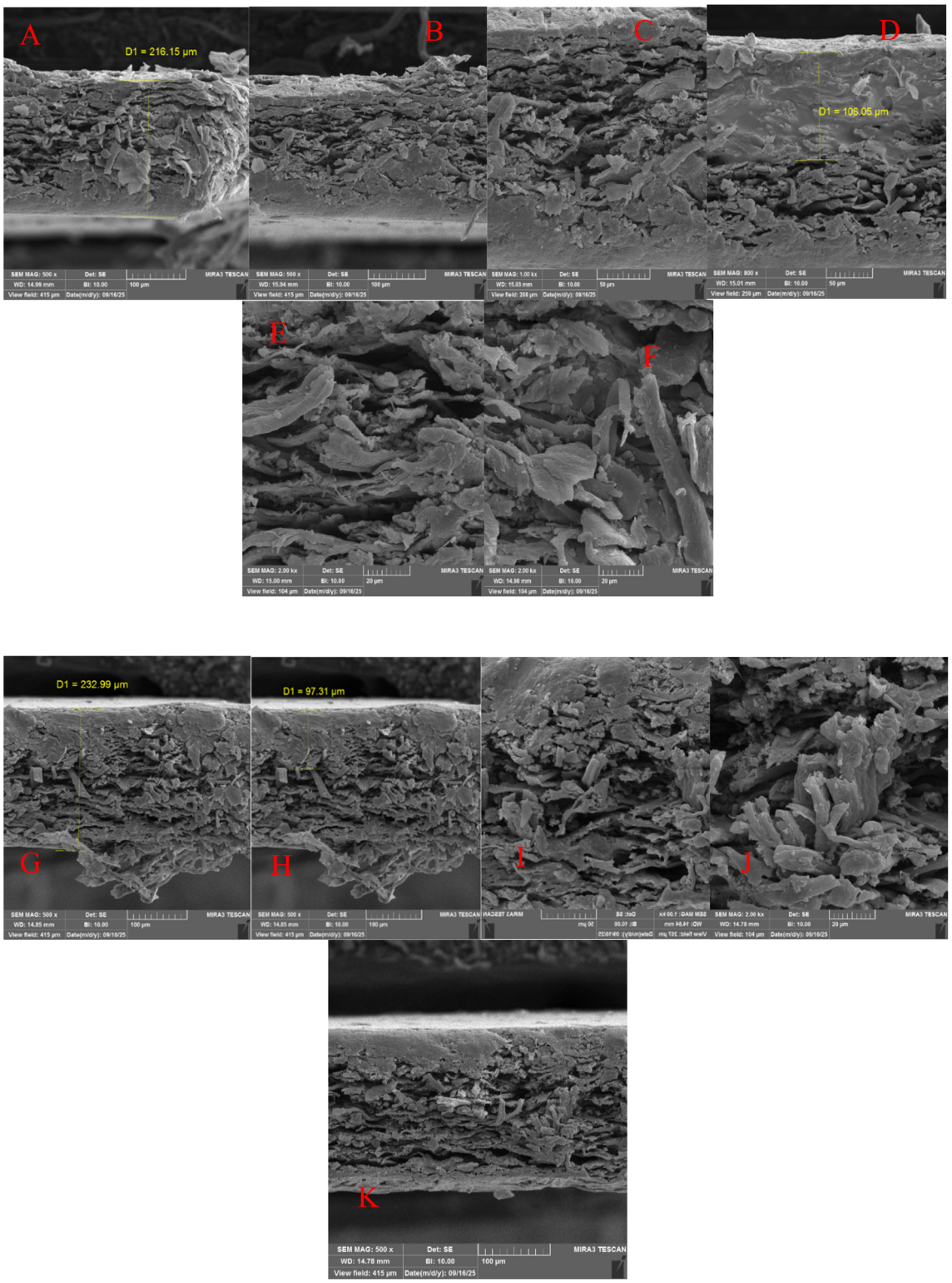

Fig. 3 (A–F) Cross-sectional FE-SEM images of the Ag nano-ink on the surface of photographic paper. (G–K) Cross-sectional FE-SEM images of the paper-based substrate decorated with EDA-Ag nano-ink at various magnifications.

other species. The results of this section show that the developed paper sensor, despite its simplicity of fabrication, has acceptable selectivity in detecting EDA. This feature is essential for applications in complex matrices such as meat extracts or plasma that contain a mixture of different organic compounds, and allows for reliable detection of the spoilage marker without the need for complex prior separation.

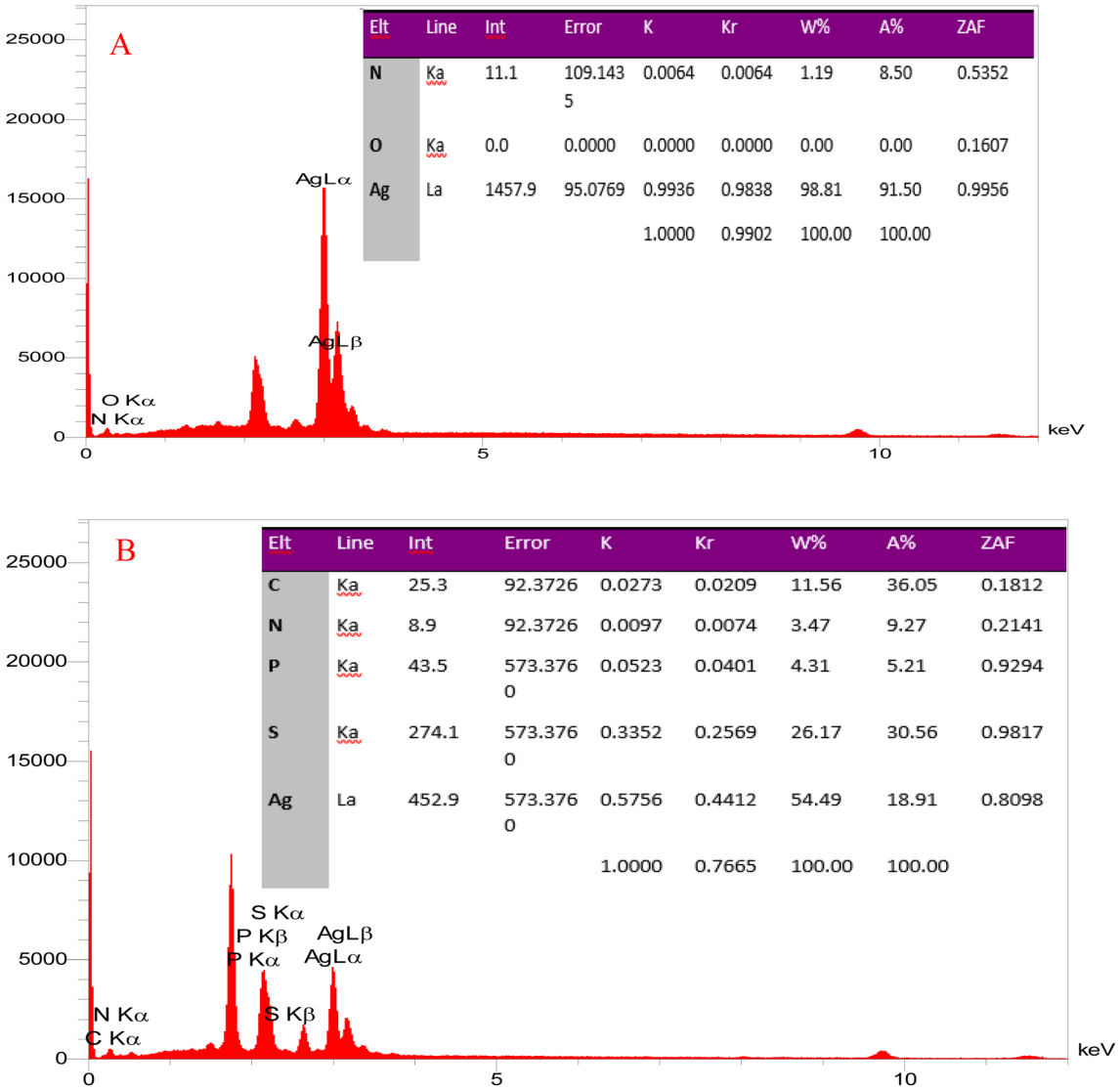

Fig. 4 (A) EDS analysis of the modified paper Ag-nano ink, and (B) EDS analysis of the modified paper EDA-Ag-nano ink on the surface of photographic paper.

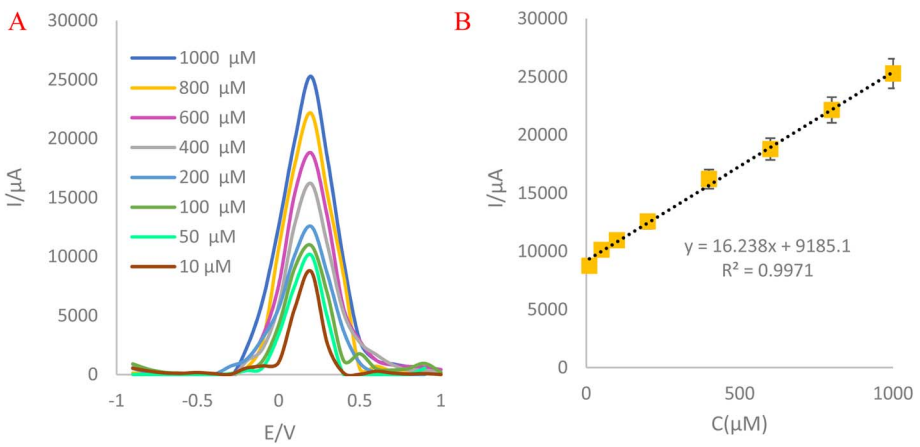

Fig. 5 (A) SWV of the paper-based electrochemical sensor using Ag nano-ink for detection of different concentrations of EDA (10, 100, 200, 400, 600, 800, and 1000 µM) in the presence of a 5 mM $[Fe(CN)_6]^{3-/4-}$/KCl solution. (B) Calibration curve obtained based on the results in (A).

Table 1 Evaluation of the sensitivity of the designed paper-based electrochemical sensor for the detection of EDA in comparison with other studies

Method	LOD or LLOQ	Linear range	Ref.
Fluorescence	42 nM	0 to 80 μM	22
	1.07 and 0.86 ppm	10 to 100 ppm	23
Electrochemical	LOD (47.4 μM) and LOQ (149 μM)	30 to 100 μM	24
Chemiresistive	0.5 ppm	0.5 to 10.0 ppm	25
	0.235 ppm	1.03 to 435.1 and 1 to 100 ppm	26
Electrochemical	94.51 nM	1 μM to 1 mM	27
Luminescence	—	—	28
Fluorescence	3.83×10^{-5} M	3.83×10^{-5} M	29
Electrochemical	3.83×10^{-5} M	0.25 to 1.25 mM	30
Electrochemical	10 μM	10 to 1000 μM	This work

3.6. Stability of the paper-based electrochemical sensor for EDA

The long-term performance of the electrodes was evaluated by measuring the changes in the electrochemical response at several time points (Fig. S5 (SI)). The storage stability of the Ag nano-ink on the paper electrode was monitored over four days using SWV voltammetry in the potential range of −1 to +1 V. Although a gradual decrease in current was observed, the results showed acceptable stability as the current response and sensor performance decreased in the following days. The decrease in the electrical response of the paper electrode could be due to gradual degradation or physical and chemical changes in the electrode structure or surface interactions between the nanoparticles and the substrate.

Also, as can be seen in Fig. 6, inter-day measurements were performed over three days for concentrations of 100, 400, and 1000 μM. The electrodes showed a notable decrease in current intensity on the third day. The corresponding standard deviation (SD) for concentrations of 100, 400, and 1000 μM was 7.33%, 7.89%, and 4.45%, respectively. The obtained results indicate that these electrodes are better for single-use applications (Table S3, SI).

Table S3 (SI) shows the evaluation of the accuracy and reproducibility of the experiment. The current values generally increased with increasing concentration. However, significant variations were observed between the experiment replicates, especially at lower concentrations. The lowest RSD% value corresponds to the highest concentration (1000 μM), indicating better measurement reproducibility under these conditions. The RSD% values are in all cases less than 10%, indicating acceptable accuracy of the measurement method in the range of concentrations studied.

3.7. Reproducibility of the paper-based electrochemical sensor in dry conditions

The reproducibility of the modified electrodes based on Ag nano-ink was determined using SWV. For this purpose, three designed electrodes were prepared for the detection of different concentrations of EDA (100, 400, and 1000 μM), and their current intensity was recorded. As shown in Fig. 7, for each concentration, the current intensity was similar, and there was no obvious difference. The current intensity, along with the SD and relative standard deviation (RSD), are listed in Table S4 (SI).

Table S4 (SI) compares the performance of the three paper-based electrochemical sensors in EDA detection. The measured current intensity clearly increased with increasing EDA concentration, indicating a concentration-dependent response of the sensors. The reproducibility of the results was

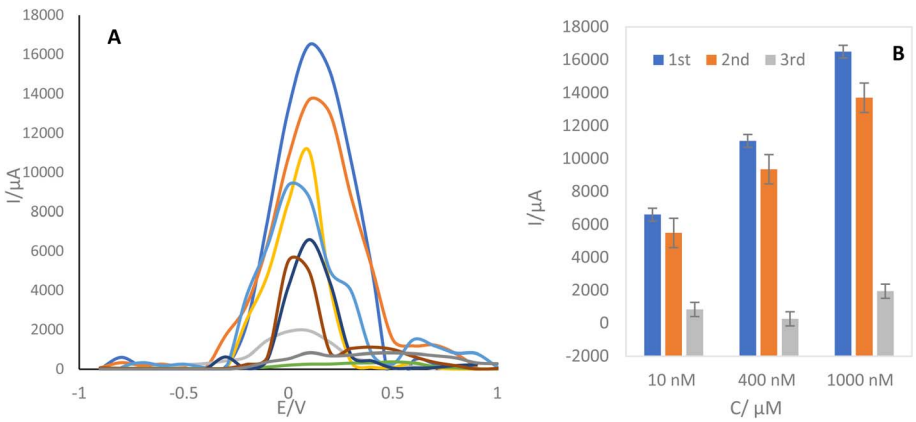

Fig. 6 (A) Three consecutive SWV scans of the three electrochemical sensors drop cast with various concentrations of EDA (100, 400, and 1000 μM). (B) Corresponding histograms for the results in (A).

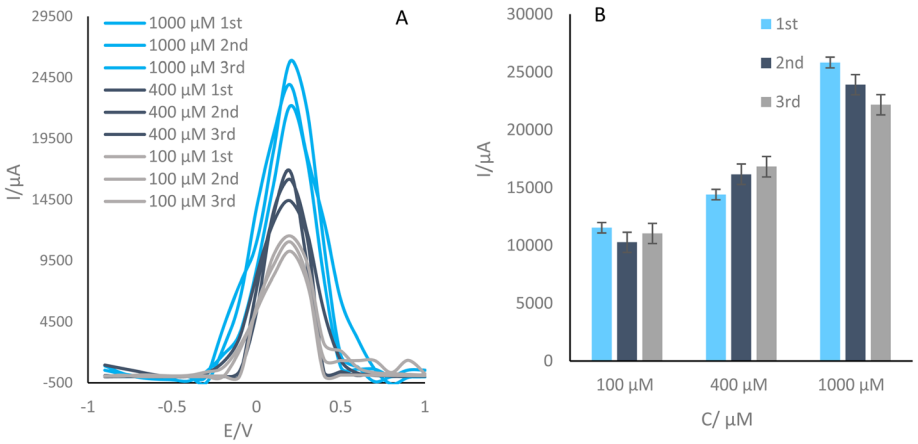

Fig. 7 (A) The SWV scans of the three paper-based electrochemical sensors with three different concentrations of EDA (100, 400, and 1000 μM). (B) Corresponding histograms for the results in (A).

evaluated by calculating the relative standard deviation (RSD%). The RSD% values for the three concentrations were 4.13%, 3.82%, and 3.64%, respectively, all of which are below 5%. This indicates excellent precision and favorable structural uniformity of the fabricated sensors. Also, the slight decrease in RSD% with increasing concentration indicates a more stable system performance at higher concentrations. Overall, the data indicate high reliability and reproducibility of this paper-based sensing platform in the studied concentration range.

4. Conclusion

In this study, a novel and affordable electrochemical sensor based on Ag ink stabilized on a paper substrate was designed for label-free detection of EDA. The application of pen-on-paper technology introduced a low-cost and simple sensing approach for the construction of the sensor. Moreover, the specific properties of EDA on the surface of the modified sensing zone improved electron transfer between the electrode and the redox species. In addition, the excellent physicochemical properties of the Ag ink enabled a selective, stable, and sensitive sensing approach. In detail, the developed three-electrode system detected EDA with a linear range of 10 to 1000 μM and a LLOQ of 10 μM. Furthermore, the high potential of the sensor for analysing EDA in real beef samples for future applications was demonstrated by its excellent analytical performance. Given the acceptable stability and reproducibility of the sensor, the developed substrate was suitable for real-world scenarios. The proposed paper-based electrochemical sensor could be improved by using a variety of bioreceptors and receptors. Additionally, modifications to the paper surface and integration with smart devices are other significant factors to consider in future work.

Conflicts of interest

There are no conflicts to declare.

Data availability

Access to the data used in this study is available upon request and may be subject to approval by the data provider. Restrictions may apply to the availability of these data, which were used under license for this study. Interested parties are encouraged to contact the corresponding author for further information on accessing the data.

Supplementary information (SI): Fig. S1: photographic images of Ag nano-ink preparation procedure. Fig. S2: EDA analysis using photographic paper-based sensor. Fig. S3: (A) SWVs of the developed electrochemica sensor in different concentrations of EDA (50, 100, 200, 400, 600, 800 and 1000 μM). (B) Calibration curves. Fig. S4: (A) SWVs of the prepared paper-based electrochemical sensor in the presence of different interferences (Glucose, Cys, AA, DA, UA, Pro, Asp, Arg, Gly and Urea). (B) Histogram of peak currents *versus* type of interferes agent. Fig. S5: (A) SWVs of paper-based electrochemical sensor over four days. (B) Histogram of peak current *versus* time of sensor incubation in dark place. Table S1: comparison of peak current and potential of different interventions. Table S2: comparison of peak current and potential of different interventions. Table S3: comparison of current intensity and RSD of three microsensors in three different concentrations. Table S4: comparison of current intensity and RSD of three paper-based electrochemical sensors in three different concentrations. See DOI: https://doi.org/10.1039/d6ra00092d.

Acknowledgements

We are grateful for financial assistance for this work from the Tabriz University of Medical Sciences' Pharmaceutical Analysis Research Center, Tabriz, Iran (78215).

References

1 J. Ashiq, U. Saeed, Z. Li and M. Nawaz, Advances in meat spoilage detection: A review of methods involving 2D-based

nanomaterials for detection of spoiled meat, *J. Food Compos. Anal.*, 2024, **132**, 106295.

2 A. N. Mafe, G. I. Edo, R. S. Makia, O. A. Joshua, P. O. Akpoghelie, T. S. Gaaz, A. N. Jikah, E. Yousif, E. F. Isoje, U. A. Igbuku, D. S. Ahmed, A. E. Essaghah and H. Umar, A review on food spoilage mechanisms, food borne diseases and commercial aspects of food preservation and processing, *Food Chem. Adv.*, 2024, **5**, 100852.

3 A. Marcobal, M. Polo, P. Martın-Alvarez and M. Moreno-Arribas, Biogenic amine content of red Spanish wines: comparison of a direct ELISA and an HPLC method for the determination of histamine in wines, *Food Res. Int.*, 2005, **38**, 387–394.

4 L. He, Z. Xu, T. Hirokawa and L. Shen, Simultaneous determination of aliphatic, aromatic and heterocyclic biogenic amines without derivatization by capillary electrophoresis and application in beer analysis, *J. Chromatogr. A*, 2017, **1482**, 109–114.

5 Y. Özogul and F. Özogul, *Biogenic amines formation, toxicity, regulations in food*, ed. B. Saad and R. Tofalo, Food Chemistry, Function and Analysis, 2019, ch. 1, pp. 1–329, DOI: 10.1039/9781788015813.

6 W. Wójcik, M. Łukasiewicz and K. Puppel, Biogenic amines: formation, action and toxicity–a review, *J. Sci. Food Agric.*, 2021, **101**, 2634–2640.

7 J. Xiong, K. Wang, Z. Yao, B. Zou, J. Xu and X.-H. Bu, Multi-stimuli-responsive fluorescence switching from a pyridine-functionalized tetraphenylethene AIEgen, *ACS Appl. Mater. Interfaces*, 2018, **10**, 5819–5827.

8 A. Önal, S. E. K. Tekkeli and C. Önal, A review of the liquid chromatographic methods for the determination of biogenic amines in foods, *Food Chem.*, 2013, **138**, 509–515.

9 P.-M. Chuang, Y.-J. Tu and J.-Y. Wu, A thiadiazole-functionalized Zn (II)-based luminescent coordination polymer with seven-fold interweaved herringbone nets showing solvent-responsive fluorescence properties and discriminative detection of ethylenediamine, *Sens. Actuators, B*, 2022, **366**, 131967.

10 H. Kholafazad-Kordasht, M. Hasanzadeh and F. Seidi, Smartphone based immunosensors as next generation of healthcare tools: Technical and analytical overview towards improvement of personalized medicine, *TrAC, Trends Anal. Chem.*, 2021, **145**, 116455.

11 J. Wu, H. Liu, W. Chen, B. Ma and H. Ju, Device integration of electrochemical biosensors, *Nat. Rev. Bioeng.*, 2023, **1**, 346–360.

12 V. C. Diculescu, A.-M. Chiorcea-Paquim and A. M. Oliveira-Brett, Applications of a DNA-electrochemical biosensor, *TrAC, Trends Anal. Chem.*, 2016, **79**, 23–36.

13 F. B. Tofighi, A. Saadati, H. Kholafazad-kordasht, F. Farshchi, M. Hasanzadeh and M. Samiei, Electrochemical immunoplatform to assist in the diagnosis of oral cancer through the determination of CYFRA 21.1 biomarker in human saliva samples: Preparation of a novel portable biosensor toward non-invasive diagnosis of oral cancer, *J. Mol. Recognit.*, 2021, **34**, e2932.

14 M. Mahmoudpour, A. Saadati, M. Hasanzadeh and H. Kholafazad-kordasht, A stretchable glove sensor toward rapid monitoring of trifluralin: a new platform for the on-site recognition of herbicides based on wearable flexible sensor technology using lab-on-glove, *J. Mol. Recognit.*, 2021, **34**, e2923.

15 L. Han, D.-P. Yang and A. Liu, Leaf-templated synthesis of 3D hierarchical porous cobalt oxide nanostructure as direct electrochemical biosensing interface with enhanced electrocatalysis, *Biosens. Bioelectron.*, 2015, **63**, 145–152.

16 M.-K. Zhang, W. Chen, M.-L. Xu, Z. Wei, D. Zhou, J. Cai and Y.-X. Chen, How buffers resist electrochemical reaction-induced pH shift under a rotating disk electrode configuration, *Anal. Chem.*, 2021, **93**, 1976–1983.

17 P. Ananthappan, M. Thangarasu and V. S. Vasantha, Effect of electrophoretic deposition for selective detection of Pb2+ ions using nitrogen and sulphur-doped reduced graphene oxide, *Microchem. J.*, 2024, **203**, 110879.

18 A. Periyasamy, S. Selvam, A. Chellakannu, V. V. Sivasamy and J. Mariakuttikan, Electrochemical Sensors for the Detection of Food Adulterants in Miniaturized Settings, *Nanosensing and Bioanalytical Technologies in Food Quality Control*, 2022, Chapter 3, pp. 139–168.

19 V. J. Ajaykumar and P. K. Mandal. Modern concept and detection of spoilage in meat and meat products, *Meat Quality Analysis, Chpter 8, Advanced Evaluation Methods, Techniques, and Technologies*, 2020,.

20 Y.-L. Tai and Z.-G. Yang, Fabrication of paper-based conductive patterns for flexible electronics by direct-writing, *J. Mater. Chem.*, 2011, **21**, 5938–5943.

21 W. Zhang, Q. Sun, Y. Zhu, J. Sun, Z. Wu and N. Tian, High-Performance Trimethylamine Sensor Based on an Imine Covalent Organic Framework, *ACS Sens*, 2024, **9**, 3262–3271.

22 Y. Ke, Y. Liu, B. Zu, D. Lei, G. Wang, J. Li, W. Ren and X. Dou, Electronic Tuning in Reaction-Based Fluorescent Sensing for Instantaneous and Ultrasensitive Visualization of Ethylenediamine, *Angew. Chem., Int. Ed.*, 2022, **61**, e202203358.

23 Y. Huang, X. Liu, Q. Wang, J. Fu, L. Zhao, Z. Liu and D. Jin, Highly responsive ethylenediamine vapor sensor based on a perylenediimide–camphorsulfonic acid complex *via* ionic self-assembly, *J. Mater. Chem. C*, 2017, **5**, 7644–7651.

24 A. Munir, A. Shah, A. H. Shah, U. A. Rana, B. Adhikari, S. B. Khan, R. Qureshi and H.-B. Kraatz, Detailed electrochemistry of the environmental toxin ethylene diamine, *J. Electrochem. Soc.*, 2014, **161**, H370.

25 S. H. Khor, R. S. H. Tan, C. Y. Kerk, M. L. Y. Lee, V. S. Lee and S. W. Phang, Sensor performance and computational study of polyaniline film in ethylenediamine detection, *Polym. Eng. Sci.*, 2024, **64**, 296–306.

26 H. Liu, J. Liu, Q. Liu, Y. Li, G. Zhang and C. He, Conductometric gas sensor based on MoO_3 nanoribbon modified with rGO nanosheets for ethylenediamine detection at room temperature, *Nanomaterials*, 2023, **13**, 2220.

27 E.-B. Kim, M. S. Akhtar, S. Ameen, A. Umar, S. Akbar and S. Baskoutas, Enhanced ethylenediamine detection using WO_3–$BiVO_4$ nanoflakes heterostructure with exceptional adsorption capabilities: experimental and theoretical studies, *Nanotechnology*, 2025, **36**, 115501.
28 P. Li, D. Yang and H. Li, Luminescence ethylenediamine sensor based on terbium complexes entrapment, *Dyes Pigm.*, 2016, **132**, 306–309.
29 Y. Kim, S.-H. Son and T. S. Lee, Detection of ethylenediamine using a fluorescent probe in solution and in a PMMA matrix, *Mol. Cryst. Liq. Cryst.*, 2014, **600**, 179–188.
30 X. Zhang, K. Li, H. Li, J. Lu, Q. Fu, Y. Jia and W. Li, Electrochemical sensing of ethylenediamine based on cuprous oxide/graphene hybrid structures, *J. Mater. Sci.*, 2015, **50**, 4288–4299.